Journal of Electromagnetic Waves and Applications, Vol. 5, No. 6, 607–622, 1991

Scattering by Rotating Optical Fibers

L. Schächter* and D. Schieber

Department of Electrical Engineering
Technion-Israel University of Technology
Haifa 32000, Israel

Abstract– Reflection from a rotating optical fiber is analyzed. It is shown that there are angles where the variation in the reflected power due to rotation is significant and it may be measurable even for relatively low angular velocities as 30 m/sec. The total variation in the reflected power is zero. We also determine the relation between the field (average) angular momentum and the (average) power carried away by each angular harmonic.

I. INTRODUCTION

Detection of accelerated motion is an essential requirement in navigation of airplanes, missiles and satellites. Until recently the mechanical gyroscope was the "heart" of such a navigation system, but for several years now it has been replaced by its optical successor. Generally speaking, the optical device operates by measuring the phase shift between two coherent anti-parallel waves which complete an entire loop when propagating in an optical fiber. Bearing in mind the Sagnac effect, it can be readily shown that this phase shift occurs due to the relative motion of the wave and the fiber, and that it is proportional to the mechanical angular frequency of the loop. This technique is not applicable in the case of very small devices, since the detection system has to accompany the moving body. An alternative method, free of the above drawback, consists of illuminating a rotating optical fiber and measuring the deviations in the spatial distribution of the reflected power. While in the first method the motion is either parallel or anti-parallel to the wave vector, here the latter is *perpendicular* to the local angular velocity and the effect of motion is mainly reflected in the electromagnetic field amplitude.

The influence of rotation of different bodies on the electromagnetic scattering process has been investigated in the past, and also quite recently [1–12]. These papers, however, were mainly concerned with the radio frequency domain, while the present study deals with the optical and sub-optical domains. In extending the frequency domain, changes across the dielectric cylinder must be taken into consideration. Accordingly, in the second section the waves reflected from a dielectric cylinder with a stepped-index cross-section are determined, while in the third the same process is analyzed for the graded-index case; these two configurations simulate some well-known optical fibers [13–16]. In the fourth section the

* Present Address: Laboratory of Plasma Studies, 369 Upson Hall, Cornell University, Ithaca, NY 14853-7501, USA.

reflected waves calculated in the second section are considered in order to establish the power and angular momentum flow. It is shown that although the spatial distribution of the scattered electromagnetic power is changed by the motion, the *total* power is conserved. A relatively simple expression for one-harmonic power and power flux-change due to the rotational motion is presented. The average angular momentum is expressed in terms of the one-harmonic average power. The feasibility of measuring this change is considered in the last section.

II. STEPPED-INDEX CROSS-SECTION

A rotating optical fiber is illuminated by an electromagnetic plane wave, and basically we are concerned with the reflection coefficient as measured by a remote observer. For a systematic solution of the problem, we adopt here a formulation resorted to in a previous communication [17]. Let us therefore define the problem more carefully:

(a) In the laboratory, we define a circular cylindrical frame of reference $S(r, \alpha, z, t)$.

(b) The dielectric cylinder, whose axis is parallel to the z-direction, rotates uniformly at the circular mechanical frequency Ω.

(c) When at rest, this cylinder is characterised by the relative dielectric coefficient

$$\epsilon(r) = \begin{cases} \epsilon_1, & 0 \leq r < R_1 \\ \epsilon_2, & R_1 < r < R_2 \end{cases} \tag{2.1}$$

and by the relative magnetic permeability unity ($\mu_r = 1$), while its electric conductivity is vanishingly small.

(d) Two additional frames of reference are now defined; a Cartesian frame $S(x, y, z, t)$ "rigidly" attached to the laboratory, and a circular cylindrical frame $S'(r', \alpha', z', t')$ "rigidly" attached to the rotating fiber. A general transformation from the rotating to the rest frame is not known. However, at today's technology the tangential speed of revolution of a macroscopic body is much smaller than the phase velocity of a plane wave in vacuum, therefore, a quasi-Galilean transformation

$$r' = r; \quad \alpha' = \alpha - \Omega t; \quad z' = z; \quad t' = t \tag{2.2}$$

may be resorted to. Further, in the rotating frame we *assume* the constitutive equations to read

$$\vec{D}' = \epsilon(r')\epsilon_0 \vec{E}' \tag{2.3}$$

along with

$$\vec{B}' = \mu_0 \vec{H}' \tag{2.4}$$

Similarly, introducing the so-called refractive index $n(r) \equiv \sqrt{\epsilon(r)}$, we *assume* for an observer stationed within the laboratory, the following constitutive relations:

$$\vec{D} = n^2 \epsilon_0 \vec{E} + (n^2 - 1) \frac{\vec{v} \times \vec{H}}{c^2} \tag{2.5}$$

$$\vec{B} = \mu_0 \vec{H} - (n^2 - 1)\frac{\vec{v} \times \vec{E}}{c^2} \tag{2.6}$$

(e) Finally, we assume that the cylinder is illuminated by a harmonic electromagnetic plane wave (circular frequency ω) of amplitude E_0 — whose electric field comprises mainly a z-component, i.e.,

$$E_z^{(p)}(x,t) = E_0 e^{-i\omega t + i\frac{\omega}{c}x} \tag{2.7}$$

the superscript p denoting the fact that this is a so-called primary wave.

The special geometry involved here favors recourse to a Bessel-Fourier series; thus in the cylindrical frame of reference $S(r,\alpha,z,t)$ the incident wave reads

$$E_z^{(p)} = E_0 \sum_{k=-\infty}^{\infty} i^k J_k\left(\frac{\omega}{c}r\right) e^{-i(\omega t - k\alpha)} \tag{2.8}$$

with the Bessel function defined as in [18]. Invoking the communication [17] referred to above, it is found that the secondary field (superscript (s)) due to the presence of the cylinder is a solution of

$$\left[\frac{\partial^2}{\partial r^2} + \frac{1}{r}\frac{\partial}{\partial r} + \frac{1}{r^2}\frac{\partial^2}{\partial \alpha^2} + \frac{\omega^2}{c^2}\right] E_z^{(s)} = 0, \qquad R_2 < r < \infty \tag{2.9}$$

$$\left[\frac{\partial^2}{\partial r^2} + \frac{1}{r}\frac{\partial}{\partial r} + \frac{1}{r^2}\frac{\partial^2}{\partial \alpha^2} + 2i\frac{\omega\Omega}{c^2}(n_2^2 - 1)\frac{\partial}{\partial \alpha} + \frac{\omega^2}{c^2}n_2^2\right] E_z^{(s)} = 0, \quad R_1 < r < R_2 \tag{2.10}$$

$$\left[\frac{\partial^2}{\partial r^2} + \frac{1}{r}\frac{\partial}{\partial r} + \frac{1}{r^2}\frac{\partial^2}{\partial \alpha^2} + 2i\frac{\omega\Omega}{c^2}(n_1^2 - 1)\frac{\partial}{\partial \alpha} + \frac{\omega^2}{c^2}n_1^2\right] E_z^{(s)} = 0, \quad 0 < r < R_1 \tag{2.11}$$

with $n_1^2 = \epsilon_1$ and $n_2^2 = \epsilon_2$.

A solution of (2.9) which obeys the Sommerfeld radiation condition at $r \to \infty$ is determined up to an unknown coefficient Γ_k and expressed by the series

$$E_z^{(s)} = E_0 \sum_{k=-\infty}^{\infty} \Gamma_k i^k H_k^{(1)}\left(\frac{\omega}{c}r\right) e^{-i(\omega t - k\alpha)} \tag{2.12}$$

where $H_k^{(1)}(\omega r/c)$ is the Hankel function of the first kind [18]; the circular magnetic field linked to this electric field reads

$$H_\alpha^{(s)} = -\frac{E_0}{\eta_0} \sum_{k=-\infty}^{\infty} \Gamma_k i^k \dot{H}_k^{(1)}\left(\frac{\omega}{c}r\right) e^{-i(\omega t - k\alpha)} \tag{2.13}$$

the dot above the Hankel function denoting its derivative with respect to its argument and $\eta_0 = \sqrt{\mu_0/\epsilon_0}$. In the domain of the dielectric cylinder, the secondary field is again determined up to three unknown coefficients, namely, A_k, B_k and T_k:

(a) For $R_1 < r < R_2$ the z-component of the electric field reads

$$E_z^{(s)} = E_0 \sum_{k=-\infty}^{\infty} (i)^k \left[A_k J_k\left(n_{k,2}\frac{\omega}{c}r\right) + B_k Y_k\left(n_{k,2}\frac{\omega}{c}r\right)\right] e^{-i(\omega t - k\alpha)} \tag{2.14}$$

while the circular component of the magnetic field is

$$H_\alpha^{(s)} = -\frac{E_0}{\eta_0}\sum_{k=-\infty}^{\infty} n_{k,2}\, i^k \left[A_k \dot{J}_k\left(n_{k,2}\frac{\omega}{c}r\right) + B_k \dot{Y}_k\left(n_{k,2}\frac{\omega}{c}r\right)\right] e^{-i(\omega t - k\alpha)} \tag{2.15}$$

The dynamic refraction coefficient defined as in [17] reads

$$n_{k,2} = \sqrt{n_2^2 - (n_2^2 - 1)\, 2k\frac{\Omega}{\omega}} \tag{2.16}$$

the dot denoting once more the derivative of the cylindrical function with respect to its argument.

(b) For $0 < r < R_1$ we consider only a solution convergent at $r = 0$; hence the z-component of the electric field reads

$$E_z^{(s)} = E_0 \sum_{k=-\infty}^{\infty} i^k T_k J_k\left(n_{k,1}\frac{\omega}{c}r\right) e^{-i(\omega t - k\alpha)} \tag{2.17}$$

whereas the circular component of the magnetic field is given by

$$H_\alpha^{(s)} = \frac{E_0}{\eta_0}\sum_{k=-\infty}^{\infty} n_{k,1}\, i^k T_k \dot{J}_k\left(n_{k,1}\frac{\omega}{c}r\right) e^{-i(\omega t - k\alpha)} \tag{2.18}$$

Once more

$$n_{k,1} = \sqrt{n_1^2 - (n_1^2 - 1)\, 2k\frac{\Omega}{\omega}} \tag{2.19}$$

The unknown coefficients Γ_k, A_k, B_k, and T_k are now determined by imposing the tangential boundary conditions at $r = R_1$ and R_2. Continuity of the z-component of the electric field at $r = R_1$ yields

$$T_k J_k(\xi) = A_k J_k(\sigma) + B_k Y_k(\sigma) \tag{2.20}$$

while that of the circular component of the magnetic field yields

$$n_{k,1}\, T_k \dot{Y}_k(\xi) = n_{k,2}\left[A_k \dot{J}_k(\sigma) + B_k \dot{Y}_k(\sigma)\right] \tag{2.21}$$

where

$$\xi = n_{k,1}\frac{\omega}{c}R_1, \qquad \sigma = n_{k,2}\frac{\omega}{c}R_1 \tag{2.22}$$

Similarly, at $r = R_2$ we have

$$J_k(\chi) + \Gamma_k H_k^{(1)}(\chi) = A_k J_k(\nu) + B_k Y_k(\nu) \tag{2.23}$$

and

$$\dot{J}_k(\chi) + \Gamma_k \dot{H}_k^{(1)}(\chi) = n_{k,2}\left[A_k \dot{J}_k(\nu) + B_k \dot{Y}_k(\nu)\right] \tag{2.24}$$

where

$$\chi = \frac{\omega}{c}R_2 \quad \text{and} \quad \nu = n_{k,2}\frac{\omega}{c}R_2 \tag{2.25}$$

The coefficient corresponding to the scattered wave is given by the ratio

$$\Gamma_k = -\frac{\dot{J}_k(\chi)[J_k(\nu) + \rho_k Y_k(\nu)] - n_{k,2} J_k(\chi)\left[\dot{J}_k(\nu) + \rho_k \dot{Y}_k(\nu)\right]}{\dot{H}_k^{(1)}(\chi)[J_k(\nu) + \rho_k Y_k(\nu)] - n_{k,2} H_k^{(1)}(\chi)\left[\dot{J}_k(\nu) + \rho_k \dot{Y}_k(\nu)\right]} \tag{2.26}$$

with

$$\rho_k = -\frac{n_{k,2}J_k(\xi)\dot{J}_k(\sigma) - n_{k,1}\dot{J}_k(\xi)J_k(\sigma)}{n_{k,2}J_k(\xi)\dot{Y}_k(\sigma) - n_{k,1}\dot{Y}_k(\xi)J_k(\sigma)} \tag{2.27}$$

all other coefficients being obtainable from (2.20)–(2.21) and (2.23)–(2.24). Obviously, (2.26)–(2.27) completely determine the reflection process; so that the influence of rotation on the radiation pattern is readily calculated.

Before proceeding to do this, let us consider a more sophisticated model of an optical fiber.

III. GRADED-INDEX CROSS-SECTION

An important member of the optical fibers group is that characterized by a graded index. In this case, when the cylinder is at rest, the dielectric coefficient may be expressed [13–16] as

$$\epsilon(r) = n^2(r) = \begin{cases} \epsilon_1 + (\epsilon_2 - \epsilon_1)(r/R)^2, & 0 \le r \le R \\ 1, & R \le r \le \infty \end{cases} \tag{3.1}$$

The secondary field in the domain of the cylinder is now a solution of

$$\left\{\frac{\partial^2}{\partial r^2} + \frac{1}{r}\frac{\partial}{\partial r} + \frac{1}{r^2}\frac{\partial^2}{\partial \alpha^2} + 2i\frac{\omega\Omega}{c^2}\left[n^2(r) - 1\right]\frac{\partial}{\partial \alpha} + \frac{\omega^2}{c^2}n^2(r)\right\}E_z^{(s)} = 0 \tag{3.2}$$

while the scattered wave is identical to that expressed in (2.12)–(2.13), except that Γ_k is now different. For the solution of (3.2) we assume the expression

$$E_z^{(s)} = E_0 \sum_{k=-\infty}^{\infty} R_k(r)\, e^{-i(\omega t - k\alpha)} \tag{3.3}$$

$R_k(r)$ being, in turn, a solution of

$$\left\{\frac{d^2}{dr^2} + \frac{1}{r}\frac{d}{dr} - \frac{k^2}{r^2} - 2\frac{\omega\Omega}{c^2}k\left[n^2(r) - 1\right] + \frac{\omega^2}{c^2}n^2(r)\right\}R_k(r) = 0 \tag{3.4}$$

Using now the explicit expression for $n^2(r)$, this last equation can be cast in the Wave-Bessel equation (as defined in [19]), namely

$$\left\{\frac{d^2}{d\rho^2} + \frac{1}{\rho}\frac{d}{d\rho} + \left[-\frac{k^2}{\rho^2} + 1 + \Delta^2\rho^2\right]\right\}R_k(\rho) = 0 \tag{3.5}$$

where

$$\rho = n_k\frac{\omega}{c}r \tag{3.6}$$

$$n_k = \sqrt{\epsilon_1 - 2k\frac{\Omega}{\omega}(\epsilon_1 - 1)} \tag{3.7}$$

$$\Delta^2 = (\epsilon_1 - \epsilon_2)\frac{1}{(\omega R n_k/c)^2}\frac{1 - 2k\Omega/\omega}{n_k^2} \tag{3.8}$$

A solution of (3.5) is now determined, as in the preceding section, i.e., up to an unknown coefficient T_k; it reads

$$R_k(\rho) = T_k\tilde{J}_k(\Delta, 1, \rho)(i)^k \tag{3.9}$$

where $\tilde{J}_k(\Delta, 1, \rho)$ is the solution of the Wave-Bessel equation and is explicitly defined in the Appendix. At the limit of a uniform dielectric coefficient $\Delta = 0$, this solution corresponds to

$$\tilde{J}_k(\Delta = 0, 1, \rho) = J_k(\rho) \tag{3.10}$$

The procedure for determining Γ_k is the same as in the preceding section, except for two technical differences:

(a) In order to calculate the circular component of the magnetic field, we have to replace in (2.17) the dynamic refraction coefficient $n_{k,1}$ by the present one, namely n_k; further, the functional dependence is also changed, i.e., $\dot{\tilde{J}}_k(n_k \omega r/c)$ instead of $\dot{J}_k(n_{k,1}\omega r/c)$.

(b) The electromagnetic properties of this system are continuous throughout space except at $r = R$; hence for a complete description it suffices to introduce only two unknown coefficients T_k and Γ_k which, in turn, may be determined by imposing the boundary conditions at $r = R$.

With the above in mind, the amplitudes of the scattered harmonics are found to read

$$\Gamma_k = -\frac{\dot{J}_k(\chi)\tilde{J}_k(\Delta, 1, n_k\chi) - n_k J_k(\chi)\dot{\tilde{J}}_k(\Delta, 1, n_k\chi)}{\dot{H}_k^{(1)}(\chi)\tilde{J}_k(\Delta, 1, n_k\chi) - n_k H_k^{(1)}\dot{\tilde{J}}_k(\Delta, 1, n_k\chi)} \tag{3.11}$$

where like in (2.25) $\chi = \omega R/c$. Once more, the reflection process is completely determined.

IV. POWER AND ANGULAR MOMENTUM CONSIDERATIONS

Knowing the amplitude of the scattered wave, we now turn our attention to the power density carried by this wave. In view of the special geometry, the only relevant component of the time-averaged power density is the radial one, which reads

$$\langle S_r \rangle = -\frac{1}{2}\,\mathrm{Re}\left\{E_z^{(s)}\left[H_\alpha^{(s)}\right]^*\right\} \tag{4.1}$$

$[\,]^*$ denoting the complex conjugate of the quantity in brackets; far away from the cylinder, this expression reduces to

$$\langle S_r \rangle = \frac{|E_0|^2}{2\eta_0}\frac{1}{\frac{\pi}{2}\frac{\omega}{c}r}\,\mathrm{Re}\left\{\sum_{m,n=-\infty}^{\infty}\Gamma_m\Gamma_n^* e^{i\alpha(m-n)}\right\} \tag{4.2}$$

The radial component of the Poynting vector determines the radiation intensity $\tilde{I}$ emitted within an angle α, $\alpha + d\alpha$ and an interval δ along the z-direction, through

$$\frac{1}{\delta}\frac{1}{r}\frac{d\tilde{I}}{d\alpha} = \langle S_r \rangle \tag{4.3}$$

The differential cross-section is determined by the dimensionless ratio

$$\frac{d\tilde{I}}{d\alpha} \equiv \frac{d\tilde{I}/d\alpha}{(|E_o|^2/2\eta_0)\delta(2R_2)} = \frac{1}{\pi(\omega R_2 c)}\,\mathrm{Re}\left\{\sum_{m,n}\Gamma_m\Gamma_n^* e^{i\alpha(m-n)}\right\} \tag{4.4}$$

Considering the effect of rotation on this quantity, we should note that assuming

$$|k|\frac{\Omega}{\omega} \ll 1 \tag{4.5}$$

(which, as we shall see later in this section, is fully justified in our analysis), the change in the refraction coefficient is quite small, namely

$$n_k \simeq n - k\left(n - \frac{1}{n}\right)\frac{\Omega}{\omega} \tag{4.6}$$

With this approximation, we find for the scattered * amplitudes

$$\begin{aligned}\Gamma_k(n_{k,1}; n_{k,2}) \simeq \Gamma_k(n_1; n_2) &- \left[n_1 - \frac{1}{n_1}\right]\frac{\Omega}{\omega}k\frac{\partial\Gamma_k}{\partial n_1}(n_1; n_2) \\ &- \left[n_2 - \frac{1}{n_2}\right]\frac{\Omega}{\omega}k\frac{\partial\Gamma_k}{\partial n_2}(n_1; n_2)\end{aligned} \tag{4.7}$$

Although we have used the parameter Ω/ω in the process of linearization, differentiation with respect to n_1 or n_2 introduces (within a good approximation) an additional term of the type $\omega R_1/c$ or $\omega R_2/c$ that multiplies n_k in the argument of the Bessel functions; hence the correction term is proportional either to $\Omega R_1/c$ or to $\Omega R_2/c$, which obviously indicates that the change in the scattered amplitude due to rotation, is proportional to the angular velocity. Accordingly, it is more convenient for our purpose to consider the corresponding change in the average power density; to this end we define the dimensionless parameter

$$s \equiv \frac{\langle S_r\rangle - \langle S_r^{(0)}\rangle}{\langle S_r^{(0)}\rangle} = -\frac{\mathrm{Re}\left\{\sum\left[\Gamma_m^{(0)}(\Gamma_n^{(1)})^* + \Gamma_m^{(1)}(\Gamma_n^{(0)})^*\right]e^{i\alpha(m-n)}\right\}}{\mathrm{Re}\left\{\sum\Gamma_m^{(0)}(\Gamma_n^{(0)})^* e^{i\alpha(m-n)}\right\}} \tag{4.8}$$

where $\Gamma_m^{(0)} = \Gamma_m(n_1; n_2)$ and $\Gamma_m^{(1)} = \frac{\Omega}{\omega}m\left[\left(\frac{n_1-1}{n_1}\right)\frac{\partial\Gamma_m^{(0)}}{\partial n_1} + \left(\frac{n_2-1}{n_2}\right)\frac{\partial\Gamma_m^{(0)}}{\partial n_2}\right]$. The last expression involves an infinite summation, and a cutoff criterion which ensures its convergence is discussed below.

Another quantity of interest is the total reflected power, whose time-averaged value reads

$$\langle P\rangle = \delta\int_0^{2\pi} d\alpha\, r\langle S_r\rangle \tag{4.9}$$

and, again, it is more convenient to consider its relative variation, namely

$$p \equiv \frac{\langle P\rangle - \langle P^{(0)}\rangle}{\langle P^{(0)}\rangle} = -\frac{\sum_m\left[\Gamma_m^{(0)}\left(\Gamma_m^{(1)}\right)^* + \left(\Gamma_m^{(0)}\right)^*\Gamma_m^{(1)}\right]}{\sum_m|\Gamma_m^{(0)}|^2} \tag{4.10}$$

This quantity vanishes *within our approximation.* In order to prove this statement we observe that $\Gamma_m^{(1)}$ is proportional to m and the term which multiplies m in the summation is an even function of this variable. The fact that no change in

* Throughout this section we refer to the stepped-index case, in the view of its mathematical simplicity.

the total scattered power occurs is not surprising: (a) because the cylinder was assumed to be made of a lossless material, and (b) because the angular velocity of the cylinder is perpendicular to the propagation wave-vector.

Since the change in the radiation power due to rotation is proportional to the angular velocity of the cylinder, it is now reasonable to investigate the average angular momentum density of the scattered EM field [20]. In order to determine the latter we have to complete the explicit description of the electromagnetic field; thus, we note that (2.12)–(2.13) describe only two of its components, the third being

$$H_r^{(s)} = \frac{E_0}{\eta_0} \sum_{k=-\infty}^{\infty} \Gamma_k \, k \, (i)^k \, \frac{H_k^{(1)}(\omega r/c)}{(\omega r/c)} \, e^{-i(\omega t - k\alpha)} \tag{4.11}$$

Accordingly, the circular component of the average Poynting vector may be expressed as

$$\langle S_\alpha \rangle = \frac{1}{2} Re \left\{ E_z^{(s)} \left[H_r^{(s)} \right]^* \right\} \tag{4.12}$$

the second component $\langle S_r \rangle$ has already been determined in (4.2), and the third component ($\langle S_z \rangle$) is identically zero.

The Poynting vector determines the momentum density of the EM field outside the cylinder domain namely $\vec{P}_f = \vec{S}/c^2$, the subscript f indicating that we are talking in field terms; thus the field angular momentum density may be now defined to read

$$\vec{L}_f = \vec{r} \times \vec{P}_f = \frac{1}{c^2} \vec{r} \times \vec{S} \tag{4.13}$$

Since the system is "infinite" in the z-direction, $\langle L_{f,z} \rangle$ is the only non-zero component of the time-averaged angular momentum density, $\langle \vec{L} \rangle$.

Next, we determine the angular momentum along the circumference of a circle of radius r; proceeding from the definition of $\langle L_{f,z} \rangle$, namely

$$\langle L_{f,z} \rangle = \frac{1}{\delta} \frac{\partial^2 L_z}{\partial x \partial y} = \frac{1}{\delta} \frac{1}{r} \frac{\partial^2 L_z}{\partial r \partial \alpha} \tag{4.14}$$

and integrating along this circle, we find that within the interval r, $r + dr$ the angular momentum per radial unit length is given by the derivative

$$\frac{dL_z}{dr} = \frac{r^2}{c^2} \delta \int_0^{2\pi} d\alpha \, \langle S_\alpha \rangle r = \frac{r^2}{c^2} \delta \frac{1}{2} \frac{E_0^2}{\eta_0} 2\pi \sum_k k |\Gamma_k|^2 \frac{|H_k^{(1)}(\omega r/c)|^2}{\omega r/c} \tag{4.15}$$

Far away from the cylinder ($r \gg R_2$) we may substitute the asymptotic expression for the Hankel function, so that the normalized angular momentum per unit length, l_z, is given by

$$l_z \equiv \frac{c \, dL_z/dr}{\frac{\epsilon_0}{2} E_0^2 (\pi R_2^2 \delta)} = \frac{4}{\pi} \frac{1}{(\omega R_2/c)^2} \sum_{k=1}^{\infty} k \left[|\Gamma_k|^2 - |\Gamma_{-k}|^2 \right] \tag{4.16}$$

the latter can be simplified if we note that (2.9)–(2.11) are invariant under replacement of α by $-\alpha$, which is equivalent to replacing k by $-k$, and Ω by

$(-\Omega)$. Hence, $\Gamma_{-k}(\Omega) = \Gamma_k(-\Omega)$. Substituting the last relations, we find for the normalized angular momentum the expression

$$l_z = \frac{4/\pi}{(\omega R_2/c)^2} \sum_{k=1}^{\infty} k \left[|\Gamma_k(\Omega)|^2 - |\Gamma_k(-\Omega)|^2 \right] \tag{4.17}$$

which emphasizes the fact that angular momentum of the field vanishes when the cylinder is at rest. The contribution to l_z, linear in Ω, reads

$$l_z = -\frac{4/\pi}{(\omega R_2/c)^2} 2\frac{\Omega}{\omega} \sum_{k=1}^{\infty} k^2 \left[\left(n_1 - \frac{1}{n_1} \right) \frac{\partial}{\partial n_1} |\Gamma_k^{(0)}|^2 + \left(n_2 - \frac{1}{n_2} \right) \frac{\partial}{\partial n_2} |\Gamma_k^{(0)}|^2 \right] \tag{4.18}$$

Somewhat deeper physical insight is achieved if we consider the total average intensity scattered by the cylinder. This quantity is readily calculated using (4.2), and reads

$$\tilde{I} \equiv \delta \int_0^{2\pi} d\alpha \, r \langle S_r \rangle = \frac{E_0^2}{2\eta_0} \delta(2\pi R_2) \frac{1}{\frac{\pi}{2}(\omega R_2/c)} \sum_k |\Gamma_k|^2 \tag{4.19}$$

It consists of the sum of the power associated with the individual harmonics, i.e., $\tilde{I} = \sum_k \tilde{I}_k$.

Let us now determine the normalized average intensity scattered by the cylinder when at rest, namely

$$\bar{I}_k \equiv \frac{\tilde{I}_k}{(E_0^2/2\eta_0)\,\delta(2R_2)} = \frac{|\Gamma_k^{(0)}|^2}{\frac{1}{2}(\omega R_2/c)} \tag{4.20}$$

Substituting this expression in (4.18), we find the field angular momentum (likewise average, normalized, per unit length), l_z, to be related to the (average and normalized) power carried away by one harmonic, through the following expression:

$$l_z = -\frac{4\Omega/\omega}{\frac{\omega}{c}R_2} \left[\left(n_1 - \frac{1}{n_1} \right) \frac{\partial}{\partial n_1} + \left(n_2 - \frac{1}{n_2} \right) \frac{\partial}{\partial n_2} \right] \sum_{k=1}^{\infty} k^2 \bar{I}_k \tag{4.21}$$

It was previously shown that the *total* electromagnetic power scattered by the cylinder is not affected by rotation of the latter. Now we have just shown that the average angular field momentum per unit length is a convenient quantity for expressing the influence of rotation on the electromagnetic field distribution.

Before concluding this section, let us consider the convergence of the expressions involving infinite summation. At a given frequency and for a specified geometry, the reflection coefficient may be approximated — resorting to corresponding expansions for Bessel functions — by the expression

$$\Gamma_k \sim \frac{1}{1 - 2j\,(e\omega R_2/2kc)^{-2k}} \tag{4.22}$$

where e is the base of natural logarithms. Now, defining $k_{co} \equiv \omega R_2 e/(2c)$, the reflection coefficient practically equals unity for $|k| < k_{co}$ and vanishes for $|k| > k_{co}$. Obviously, there is a sharp cutoff at

$$|k| \sim k_{co} \tag{4.23}$$

whereby the infinite summations become finite, ensuring convergence of all expressions derived above. This cutoff, determined on the basis of information for an ideally conducting cylinder, is a supremum and will in any case be smaller for a dielectric material.

Finally, the inequality in (4.5) may now be estimated: substituting (4.23) we observe that the correction term in (4.6) is proportional to the angular velocity

$$\left(k\frac{\Omega}{\omega}\right)_{\max} = \left(\frac{\omega}{c}R_2\frac{e}{2}\right)\frac{\Omega}{\omega} \sim \frac{\Omega}{c}R_2 \ll 1 \tag{4.24}$$

which is smaller than unity by at least 4 orders of magnitude for any macroscopic body of interest.

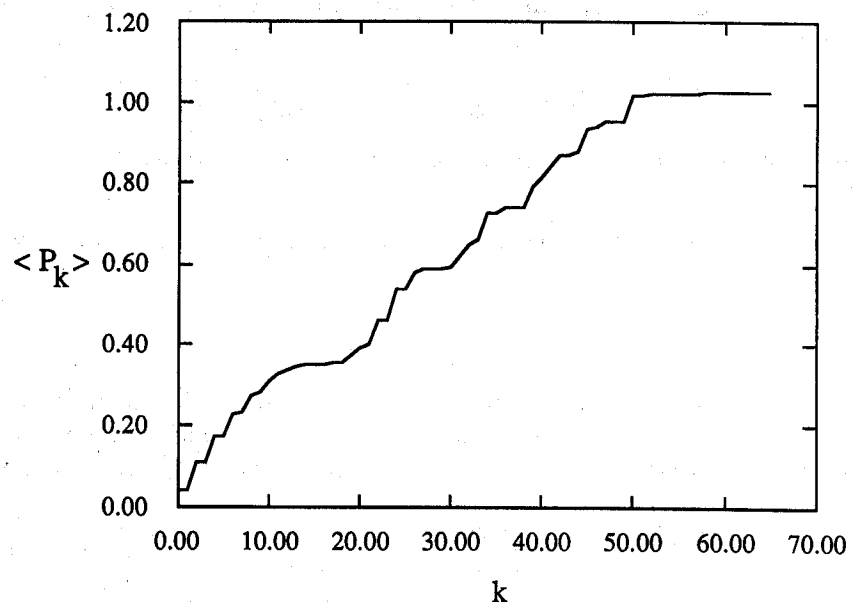

Figure 1. "Cumulative" contribution of spatial harmonics to normalized scattered power. Above $k \simeq 50$ the contribution is negligible and $\langle P^{(0)}\rangle/P_0$ equals unity.

V. NUMERICAL EXAMPLE

Construction of electro-mechanical micro-devices is feasible today by means of standard VLSI techniques (e.g., [21]). Because of their size (order of microns!), it will be quite difficult in the future to measure the angular velocity of such devices by mechanical or electrostatic methods. A possible "non-destructive" solution (in the sense that the main process is not significantly affected during the measurement) may be based on the analysis just put forward; an additional advantage is that, in principle, both the illumination source (the laser) and the detectors can be set up in close proximity to the device.

In the remainder of this communication we consider a typical device, and the feasibility of measuring the influence of rotation on the scattered field is demonstrated numerically.

To illustrate this influence in the case of a stepped-index dielectric cylinder, we consider values of $\omega R_2/c = 50$ and $\omega R_1/c = 25$ (e.g., $\lambda \sim 10\,\mu$m and $R_2 \sim 0.1$ mm). For communication applications of optical fibers it is necessary to minimize the dispersion and the refraction coefficients n_1 and n_2 have to be as close as possible to unity; this however is not the case here, and we take $n_1 = 4.0$ and $n_2 = 2.0$. In order to estimate the frequency ratio Ω/ω, we assume the normalized angular velocity to be very small, namely, $(\Omega/c)R_2 \sim 10^{-5}$ so that finally we arrive at a case for which $\Omega/\omega = 10^{-6}$.

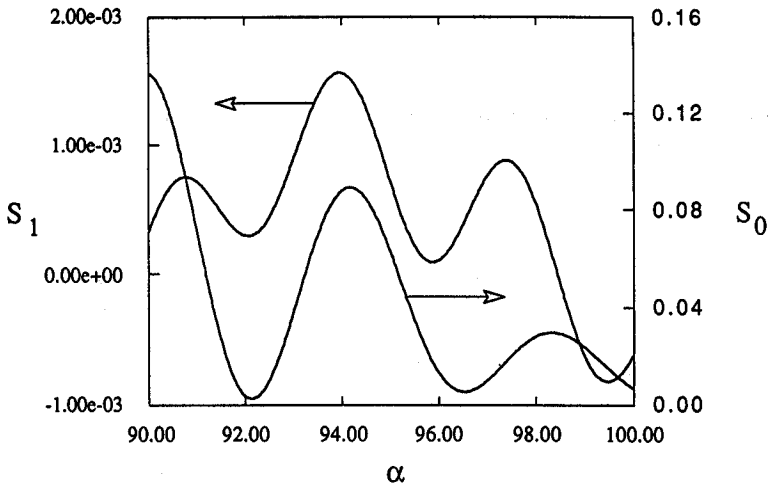

Figure 2. Angular distribution of normalized scattered flux S_0 and its corresponding change S_1.

As first step, let us demonstrate that the reflection as calculated for the cylinder at rest, is not affected by summing a large number of rapidly varying (Bessel) functions. The effective surface of the cylinder "seen" by the incident wave is $\delta(2R_2)$; the initial average power impinging on the cylinder is therefore $\langle P_0\rangle = (E_0^2/2\eta_0)\delta(2R_2)$. If we now normalize the average scattered power with respect to this quantity, we expect by virtue of energy conservation that

$$\frac{\langle P^{(0)}\rangle}{\langle P_0\rangle} = \frac{2}{\omega R_2/c}\sum_{k=-\infty}^{\infty}|\Gamma_k^{(0)}|^2 \tag{5.1}$$

should be exactly unity. In Fig. 1, we describe the "accumulation" process as each harmonic k is added, i.e., we plot $\langle P_k\rangle \equiv \dfrac{2}{(\omega/c)R_2}\sum_{m=-k}^{k}|\Gamma_m^{(0)}|^2$ as function of k. Noting that the contribution of the harmonics with index above 50 is negligible in accordance with the cutoff criterion in the preceding section, we take in the sequel $k_{\max} = 65$.

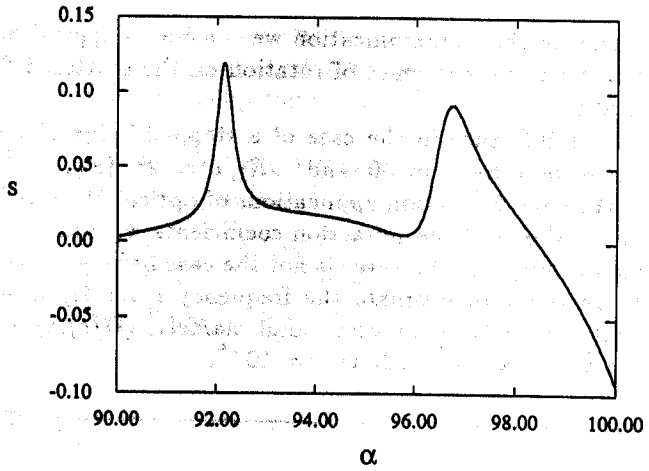

Figure 3. Angular distribution of relative change of scattered flux, s (see (4.8)), $\alpha = 90°$–$100°$.

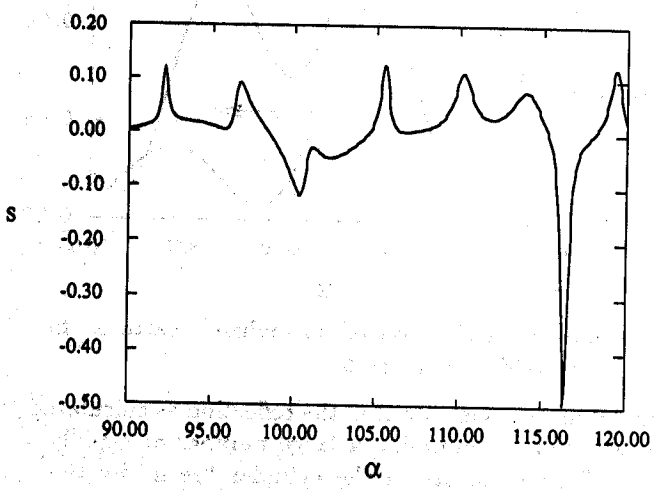

Figure 4. Angular distribution of relative change of scattered flux $\alpha = 90°$–$120°$.

Now we can consider the angular distribution of the average power flux, $\langle S_r \rangle$ and its variation due to rotation. These two quantities are described in Fig. 2, one curve referring to $S_0 \equiv \langle S_r^{(0)} \rangle (r/R_2)\delta(2R_2)/\langle P_0 \rangle$ and the other line — the corresponding change of the scattered power $S_1 \equiv \langle S_r^{(1)} \rangle (r/R_2)\delta(2R_2)/\langle P_0 \rangle$, within a limited interval of α. We observe that S_0 has minima at different angles, hence the influence of rotation is brought out when considering the relative change in the power flux (s of (4.8)). This is clearly illustrated in Fig. 3, where we present two peaks of s; a relative change of 12.5% is measurable at 92° and almost 10% near 97°. The higher peak (−50%) was calculated near $\alpha = 116°$ where S_0 is very

small — see Fig. 4. The smoothness of S_1 as presented in Fig. 2 is misleading; it is mainly due to the limited angular interval chosen. When the latter is extended, the picture changes — see e.g., Fig. 5. In spite of this "noisy" behavior, when the sum of all the contributions is taken around the cylinder, the result is closer to zero than might be expected, namely p (see (4.10)) was found to be 10^{-15} while the calculation error in evaluating the zero-order Bessel function is of order 10^{-8} — see [19].

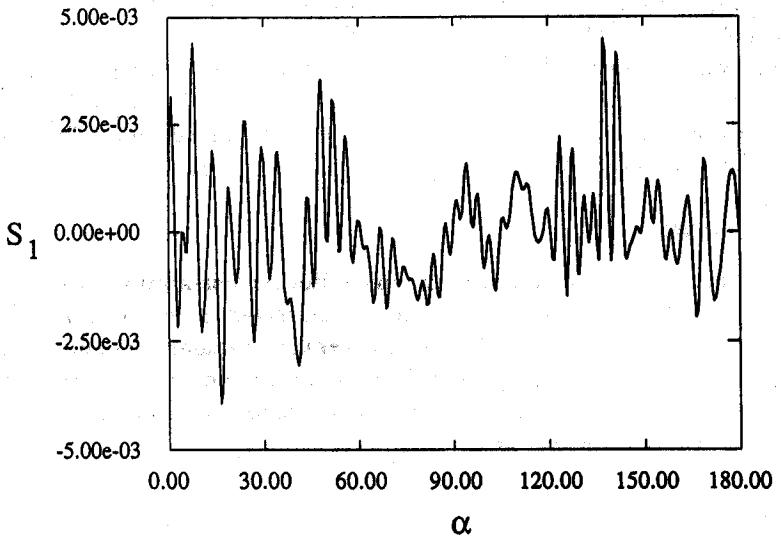

Figure 5. Angular distribution of relative change of scattered flux $\alpha = 0°$–$180°$.

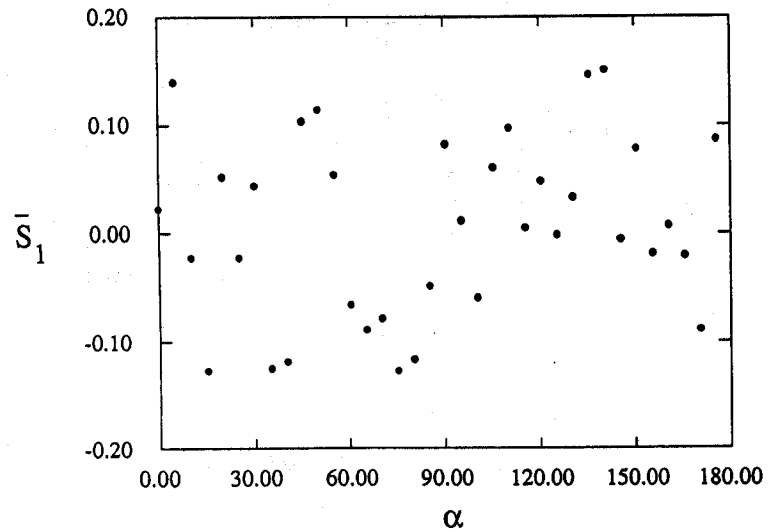

Figure 6. Relative change of scattered power at 5° interval $\alpha = 0°$–$175°$.

Let now an array of detectors measure the electromagnetic power emitted over angular intervals of 5°. The dots in Fig. 6 illustrate the accumulated normalized change of the scattered power due to rotation, $\bar{S}_1(\alpha) \equiv \int_{\alpha}^{\alpha+5^\circ} d\alpha' S_1(\alpha')$, as determined by this array. Note that this diagram reproduces the absolute variation not the relative one as in Fig. 3. Our calculations reveal that the largest change corresponds to the interval between 140° and 145°: +15.09%; a similar result (+14.7%) is obtained at $135^\circ < \alpha < 140^\circ$. For other intervals the change may be negative, e.g., for $75^\circ < \alpha < 80^\circ$, $\overline{S}_1 = -12.56\%$ and $80^\circ < \alpha < 85^\circ$, $\overline{S}_1 = -11.65\%$.

From the values presented above, we realize that even the angular velocity is decreased by two orders of magnitude, i.e., $(\Omega/c)R_2 \sim 10^{-7}$ and $\Omega/\omega = 10^{-8}$, we still obtain a change of order of 0.1% in the normalized power flux, which is within the limit of detection.

VI. CONCLUSIONS

Reflection from a rotating cylinder with non-uniform cross-section was considered; it was shown that the total variation in the reflected power is zero. We also determined the relation between the field (average) angular momentum and the (average) power carried away by each angular harmonic. Finally, it was shown that the change in the distributed power flux is measurable even for relatively low angular velocities as $\Omega R_2/c \sim 10^{-7}$.

APPENDIX

The expression for $\tilde{J}_k(\delta, q, s, \rho)$ (tabulated in [19], p. 173) is given by

$$\tilde{J}_k(\Delta, q) = [q\rho/2]^k \sum_{m=0}^{\infty} \frac{(-)^m d_m^{(k)} \left(\frac{\rho}{2}\right)^{2m}}{m!(m-k)!}$$

with

$$d_m^{(k)} = \begin{Bmatrix} q^2 & [2] & 0 & \dots & 0 & 0 & 0 \\ \Delta^2 & q^2 & [4] & \dots & 0 & 0 & 0 \\ 0 & \Delta^2 & q^2 & [6] & 0 & 0 & 0 \\ \cdot & \cdot & \cdot & \cdots & \cdot & \cdot & \cdots \\ \cdot & \cdot & \cdot & \cdots & \cdot & \cdot & \cdot \\ 0 & 0 & 0 & \dots & \Delta^2 & q^2 & [2(m-1)] \\ 0 & 0 & 0 & \dots & 0 & \Delta^2 & q \end{Bmatrix}$$

where

$$[2] = [(k+2)^2 - k^2] = 4(k+1)$$
$$[4] = [(k+4)^2 - k^2] = 8(k+2)$$
$$\vdots$$
$$[2m] = [(k+m)^2 - k^2] = 4m(k+m)$$

Explicitly, the first terms of the power-series expansion read

$$\tilde{J}_k(\Delta, q, \rho) = \frac{(q\rho/2)^k}{k!}$$
$$\left\{1 - \frac{(q\rho/2)^2}{1!(k+1)} + \frac{(q\rho/2)^4\left[1 - 4(k+1)\frac{\Delta^2}{q^2}\right]}{2!(k+1)(k+2)} - \frac{(q\rho/2)^6\left[1 - 4(3k+5)\frac{\Delta^2}{q^4}\right]}{3!(k+1)(k+2)(k+3)} \cdots\right\}$$

Comparing (3.5) with the corresponding equation in [19] (p. 172, (7.28)), it is readily seen that in our case $q = 1$.

ACKNOWLEDGMENT

The Editor thanks T. Shiozawa, and two anonymous Reviewers for reviewing the paper.

REFERENCES

1. Tai, C. T., "Two scattering problems involving moving media," Ohio State Univ. Res. Found., Rept. 1691–7, 1964.
2. Van Bladel, J., "Relativistic theory of rotating disks," *Proc. IEEE,* Vol. 61, 260–268, 1973.
3. Shiozawa, T., "Phenomenological and electron-theoretical study of the electrodynamics of rotating systems," *Proc. IEEE,* Vol. 61, 1964–1702, 1973.
4. Shiozawa, T., and K. Tanaka, "Scattering of electromagnetic waves by a rotating dielectric column," *Electr. Comm. Japan,* Vol. 57–B, 67–72, 1974.
5. Seikai, S., and T. Shiozawa, "Scattering of electromagnetic waves by a rotating electron plasma column," *IEEE Trans. Antennas Propagat.,* Vol. AP–23, 75–83, 1975.
6. Van Bladel, J., "Electromagnetic fields in the presence of rotating bodies," *Proc. IEEE,* Vol. 64, 301–318, 1976.
7. Goto, H., and T. Shiozawa, "Relativistic solution to the problem of scattering by a rotating dielectric column," *J. Appl. Phys.,* Vol. 49, 556–561, 1978.
8. Chuang, C. W., "Backscatter of a large rotating conducting cylinder of arbitrary cross section," *IEEE Trans. Antennas Propagat.,* Vol. AP–27, 92–95, 1979.
9. De Zutter, D., "Scattering of a rotating dielectric sphere," *IEEE Trans. Antennas Propagat.,* Vol. AP–28, 643–651, 1980.
10. De Zutter, D., "Scattering by a rotating circular cylinder with finite conductivity," *IEEE Trans. Antennas Propagat.,* Vol. AP–31, 166–169, 1983.
11. De Zutter, D., and D. Goethals, "Scattering by a rotating conducting sphere," *IEEE Trans. Antennas Propagat.,* Vol. AP–32, 95–98, 1984.
12. Van Bladel, J., *Relativity and Engineering,* Springer, Berlin, 1984.
13. Olshansky, R., and D. B. Keck, "Pulse broadening in graded-index optical fibers," *Applied Optics,* Vol. 15, 483–491, 1976.
14. Ankiewicz, A., and C. Pask, "Geometric optics approach to light acceptance and propagation in graded index fibers," *Opt. Quant. Elect.,* Vol. 9, 87–109, 1977.
15. Giallorenzi, T. G., "Optical communications research and technology: fiber optics," *Proc. IEEE,* Vol. 66, 744–780, 1978.
16. Gloge, D., "Optical fiber theory: opportunity for advancement abound," *Radio Science,* Vol. 12, 479–490, 1977.
17. Schieber, D., "Some remarks on scattering by a rotating dielectric cylinder," *J. Electro. Waves Applic.,* Vol. 2, 155–169, 1987.

18. Abramowitz, M., and I. Stegun, *Handbook of Mathematical Functions,* Dover Publications Inc., New York, 1968.
19. Moon, P., and D. E. Spencer, *Field Theory Handbook,* Springer, Berlin, 1961.
20. Haus, H. A. and H. Kogelnik, "Electromagnetic momentum flow in dielectric waveguides," *J. Opt. Soc. Am.,* Vol. 66, 320–327, 1976.
21. Anderson, I., "Motors no wider than a human hair," *New Scientist,* Vol. 119, 44, 1988.

Levi Schächter completed his D.Sc. in 1988 at the Electrical Engineering Department, Technion–Israel Institute of Technology and he continued there as lecturer; at present Dr. Schächter is with the Laboratory of Plasma Studies at Cornell University. His fields of interest are: sources of coherent radiation, macroscopic electrodynamics and electromagnetic theory.

David Schieber received the D.Sc. degree from the Technion-Israel Institute of Technology in 1965. Since 1976 he has been Professor of Electrical Engineering at the Technion; he has also served as Visiting Professor at various universities in Israel, in Europe and in the U.S.A. His field of interest is electromagnetism.